Tight-binding molecular-dynamics study of phonon anharmonic effects in silicon and diamond

C. Z. Wang
Department of Physics and Microelectronics Research Center, Iowa State University, Ames, Iowa 50011-3020

C. T. Chan
Ames Laboratory–U.S. Department of Energy, Ames, Iowa 50011-3020

K. M. Ho
Department of Physics and Microelectronic Research Center, Iowa State University, Ames, Iowa 50011-3020 and Ames Laboratory–U.S. Department of Energy, Ames, Iowa 50011-3020

(Received 19 April 1990)

The anharmonic effects on phonons in silicon and diamond have been studied by molecular-dynamics simulations using an empirical tight-binding Hamiltonian. One-phonon spectral intensities of the zone-center and zone-boundary (X) modes have been calculated through the Fourier transform of the velocity-velocity correlation functions. This scheme allows a quantitative and nonperturbative study of phonon frequency shift and phonon linewidth as a function of temperature. The results obtained are in good agreement with experimental data.

I. INTRODUCTION

The temperature dependence of phonon frequency shifts and phonon linewidths in semiconductors have been studied by both light-scattering as well as neutron-scattering techniques.[1] On the theoretical side, calculations on phonon frequency shifts and phonon linewidths in these systems have been restricted to perturbative approaches, where anharmonic coupling constants are usually derived either by fitting to experimental data,[2,3] or more recently, extracted from the first-principles total-energy calculations.[4] Due to the complexity of the calculation, perturbation expansion is practical only for lowest orders (rarely beyond fourth order in the force constants). For strongly anharmonic systems or systems at high temperatures, the perturbation approach becomes unsatisfactory.

In order to provide a better alternative, we have undertaken a nonperturbative approach where the observable dynamical quantities related to anharmonic effects are derived from time correlation functions in molecular-dynamics simulations. While molecular dynamics is the method of choice in handling the temperature and pressure dependence of atomic motion, the success of the approach depends on the availability of realistic interatomic interactions which must give an accurate description of the anharmonic coupling of the system and yet is simple enough so that the simulation can be carried out for a reasonably large ensemble of atoms for a large number of time steps. Conventionally, molecular dynamics is performed with empirically determined classical potentials, which in most cases consist of pair, and in some cases triplet interatomic interactions. Such potentials contain a set of parameters to be determined usually by fitting to experimental data. There are very few systems where the interatomic interactions, particularly the anharmonic interactions, can be accurately and uniquely determined by such a fitting procedure. Very few studies on anharmonic effects in solids using molecular dynamics have been reported. Previous studies of anharmonic effects using molecular dynamics have been restricted to cases where the interatomic interaction is adequately described by simple pair potentials as in the case of the alkali metals[5] and rare-gas solids.[6]

Recently, we have developed a molecular-dynamics (MD) scheme[7,8] in which the interatomic forces acting on the atoms are derived using a tight-binding force model. This scheme includes the quantum-mechanical multiatom nature of the covalent bonding present in semiconductors through explicit evaluation of the electronic structure of the system at each step in the MD simulation. The total energy of the system is described as the sum of two terms: a band-structure energy arising from the sum of all the occupied electronic eigenvalues and a term due to short-ranged pairwise interactions between atoms. The parameters of our model are determined from first-principles band-structure and total-energy calculations without any fitting to experimental data. We note that Khan and Broughton[9] have developed a similar scheme using a different algorithm for solving the electronic structure.

The purpose of this paper is to show that our tight-binding molecular-dynamics (TBMD) scheme is very useful for studying anharmonic effects in silicon and carbon in the diamond structure. In Sec. II, we will outline the TBMD scheme and the tight-binding force model for silicon and diamond. Details of the calculations are given in Sec. III. Our results on temperature-dependent phonon frequency shifts and phonon linewidths in silicon and in diamond are presented in Sec. IV. Finally, some discussions on our TBMD scheme in comparison with other schemes for studying the phonon anharmonic effects in solids will be given in Sec. V.

II. TIGHT-BINDING MOLECULAR-DYNAMICS SCHEME

The basic idea of the TBMD scheme is to incorporate the electronic effects into molecular dynamics through an empirical tight-binding Hamiltonian. In this scheme, the binding energy E_{bind} of the system is expressed as

$$E_{\text{bind}} = E_{bs} + \sum_{j>i} \phi(r_{ij}) + \text{const} , \tag{1}$$

where E_{bs} is the quantum-mechanical bond energy evaluated by summing over all occupied electronic band energies ε_n from the empirical tight-binding calculation. $\phi(r)$ is a pair potential representing the ion-ion interaction and the correction for double counting the electron-electron interaction in E_{bs}.

The details of the TBMD scheme have already been discussed in an earlier paper.[7] We use a nearest-neighbor orthogonal tight-binding model with a minimal basis set of sp^3 orbitals to describe the electronic structure in silicon and diamond. The tight-binding parameters consist of two on-site energies and four hopping parameters for each material. These parameters are chosen from the previous work by Chadi[10] and by Chadi and Martin[11] as listed in Table I. The distance dependence of the hopping parameters is assumed to be r^{-2} as proposed by Harrison.[12]

The pair potential $\phi(r)$ in Eq. (1) extends to the nearest neighbors for both Si and C. Once we have determined the tight-binding parameters, the band structure part of the binding energy as a function of the nearest-neighbor distance for the ideal diamond structure $E_{bs}^{(0)}(r)$ can be calculated. The pair potential is then determined by subtracting $E_{bs}^{(0)}(r)$ from the first-principles local-density-approximation (LDA) results of the binding energy as a function of nearest-neighbor distance for the ideal diamond structure $E_{\text{bind}}^{(0)}(r)$, which can be found in the literature.[13,14] $E_{\text{bind}}^{(0)}(r)$ can be described very well by a universal binding curve[15] and $E_{bs}^{(0)}(r)$ can be fitted with a polynomial,

$$E_{\text{bind}}^{(0)}(r) = E_0 \left[1 + \frac{(r - r_0)}{A} \right] e^{-(r-r_0)/A} \tag{2a}$$

and

$$E_{bs}^{(0)} = \sum_{l=0}^{5} C_l (r - r_c)^l . \tag{2b}$$

We have an analytic form for the pair potential $\phi(r)$ as

TABLE I. Empirical tight-binding parameters for Si and C.

Parameters	Si	C
E_s (eV)	−5.25	−2.99
E_p (eV)	1.20	3.71
$V_{ss\sigma}$ (eV)	−1.938	−5.55
$V_{sp\sigma}$ (eV)	1.745	5.91
$V_{pp\sigma}$ (eV)	3.050	7.78
$V_{pp\pi}$ (eV)	−1.075	−2.50

TABLE II. Value of the parameters in Eqs. (2a) and (2b) for silicon and diamond.

Parameters	Silicon	Diamond
E_0 (eV)	−4.8060	−7.8410
r_0 (Å)	2.3627	1.5409
A (Å)	0.5076	0.3650
r_c (Å)	2.20	1.40
C_0 (eV)	−23.37	−53.86
C_1 (eV/Å)	17.32	87.286
C_2 (eV/Å^2)	−12.42	−94.403
C_3 (eV/Å^3)	5.25	88.906
C_4 (eV/Å^4)	0.00	−72.872
C_5 (eV/Å^5)	0.00	38.516
const (eV)	11.15	20.22

$$\phi(r) = \tfrac{1}{2}[E_{\text{bind}}^{(0)}(r) - E_{bs}^{(0)}(r) - \text{const}] . \tag{2c}$$

The value of the parameters in (2) for Si and diamond are listed in Table II. This procedure guarantees that the volume dependence of the binding eneryg in our model reproduces that of the LDA results if the crystal stays in the diamond structure.

As one can see from Tables III and IV, the tight-binding force model yields good elastic properties and phonon frequencies for Si and diamond at $T = 0$ K when compared with experimental data and first-principles calculations. In particular, the good agreement between the present calculation and experimental values for the mode Grüneisen parameters indicates that we are modeling the anharmonic interactions correctly. We will demonstrate in the following that this model, although simple, has sufficient accuracy for the simulation of anharmonic effects of Si and C in the diamond structure.

III. SIMULATION DETAILS

Molecular-dynamics simulations were performed with 64 Si (and C) atoms enclosed in a cubic "box." The volume of the MD cells are fixed at a given temperature according to the lattice thermal expansion given by the same tight-binding model potentials.[7] The atoms are initially arranged in the diamond structure with small random displacements to start the simulation. Periodic boundary conditions are imposed in all three directions. The forces are updated for every MD step along with the electronic band structure, which we find by diagonalizing the tight-binding Hamiltonian. The equations of motion for the atoms are solved by a fifth-order predictor-corrector algorithm with a time step of $\Delta t = 1.07 \times 10^{-15}$ s for silicon and $\Delta t = 0.7 \times 10^{-15}$ s for diamond. Since the electronic degrees of freedom are not explicitly involved in the dynamics, the simulation time steps used are similar to those in traditional molecular-dynamics simulations. The choice of time step Δt in the present simulations conserved the total energy to within 3.9×10^{-6} and 8.1×10^{-5} eV, respectively, for silicon and for diamond over 16 400 MD steps at a simulation temperature of 100 K.

The phonon anharmonic effects were studied through

TABLE III. $T=0$ K equilibrium properties of silicon obtained by the present tight-binding model are compared with the first-principles calculation results and with experiment. The first-principles results are taken from Refs. 13 and 16. The experimental data are quoted from Ref. 1.

	Tight-binding	LDA	Experiment
a_0 (Å)	5.456	5.456[a]	5.44
B (10^{11} erg/cm^3)	9.20	9.20[a]	9.78
$C_{11}-C_{12}$ (10^{11} erg/cm^3)	7.25	9.80[b]	10.12
C_{44}^0 (10^{11} erg/cm^3)	10.26	11.10[b]	
C_{44} (10^{11} erg/cm^3)	6.16	8.50[b]	7.96
LTO(Γ) (THz)	16.95	15.16[a]	15.53
TA(X) (THz)	4.96	4.45[a]	4.49
TO(X) (THz)	14.71	13.48[a]	13.90
LOA(X) (THz)	12.37	12.16[a]	12.32
$\gamma_{\mathrm{LTO}(\Gamma)}$	0.98	0.92[a]	0.98
$\gamma_{\mathrm{TA}(X)}$	−1.12	−1.50[a]	−1.40
$\gamma_{\mathrm{TO}(X)}$	1.37	1.34[a]	1.50
$\gamma_{\mathrm{LOA}(X)}$	1.02	0.92[a]	0.90

[a]Reference 13.
[b]Reference 16.

the temperature dependence of one-phonon spectral intensities, which were calculated as Fourier transforms of velocity-velocity correlation functions in the course of the molecular-dynamics simluation.[17] Namely,

$$g(\mathbf{k},\omega)=\int dt\, e^{i\omega t}\sum_n e^{-i\mathbf{k}\cdot\mathbf{R}_n}\left[\frac{\langle \mathbf{v}_n(t)\cdot\mathbf{v}_0(0)\rangle}{\langle \mathbf{v}_n(0)\cdot\mathbf{v}_0(0)\rangle}\right], \quad (3)$$

where $\mathbf{v}_n(t)$ is the velocity of the nth atom at time t, $\mathbf{R}_n$ is the lattice position of the nth atom, and $\mathbf{k}$ is the phonon wave vector. With $\mathbf{k}=(2\pi/a)(1,1,1)$ and $(2\pi/a)(1,0,0)$, we have studied the optical phonon at the center of the Brillouin zone [LTO(Γ)] and both optical and acoustic phonons at the zone-boundary wave vector X, i.e., TO(X), LOA(X), and TA(X) for Si and diamond, respectively. The typical output of phonon spectral intensities of diamond at these two wave vectors is shown in Fig. 1, where the positions of the resonant peaks represent the frequencies of the corresponding phonon modes and the half-width of the peaks is related to the lifetime of the modes. The optical mode at Γ, i.e., LTO(Γ) and both the acoustic and optical modes at X, i.e., the TA(X), LOA(X), and TO(X) modes are well defined in the spectra. The phonon spectral densities for Si are similar and have been reported in earlier publications.[7,8]

At each temperature, we typically run 8000 MD steps to equilibrate the system, followed by another 16 384 MD steps (corresponding to a total time period of 17.5 ps) for Si and 32 768 MD steps (corresponding to a total time period of 23 ps) for diamond to evaluate the velocity-velocity correlation functions and phonon spectral intensities. The frequency resolutions ($\sim$1.0 cm^{-1} for Si and $\sim$0.8 cm^{-1} for diamond) of the calculated phonon spectra are comparable with those of typical optical experiments.

Since molecular-dynamics simulations follow the rules

TABLE IV. $T=0$ K equilibrium properties of diamond obtained by the present tight-binding model are compared with the first-principles calculation results and with experiment. The first-principles results are taken from Ref. 14. The experimental data are quoted from Ref. 1.

	Tight-binding	LDA	Experiment
a_0 (Å)	3.56	3.56	3.567
B (10^{11} erg/cm^3)	4.37	4.37	4.42
$C_{11}-C_{12}$ (10^{11} erg/cm^3)	80.92		95.12
C_{44}^0 (10^{11} erg/cm^3)	52.71		
C_{44} (10^{11} erg/cm^3)	48.13		57.74
LTO(Γ) (THz)	45.38	40.10	39.96
TA(X) (THz)	24.96		24.21
TO(X) (THz)	35.80		32.07
LOA(X) (THz)	38.02		35.55
$\gamma_{\mathrm{LTO}(\Gamma)}$	0.95		0.96
$\gamma_{\mathrm{TA}(X)}$	0.06		
$\gamma_{\mathrm{TO}(X)}$	1.45		
$\gamma_{\mathrm{LOA}(X)}$	0.89		

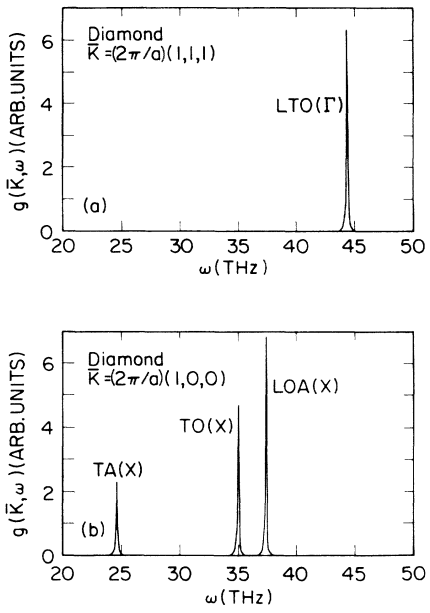

FIG. 1. Typical TBMD phonon spectral intensity of diamond calculated by Eq. (3) and with (a) $\mathbf{k}=(2\pi/a)$ (1,1,1) and (b) $\mathbf{k}=(2\pi/a)$ (1,0,0). The simulation temperature is $T=597$ K.

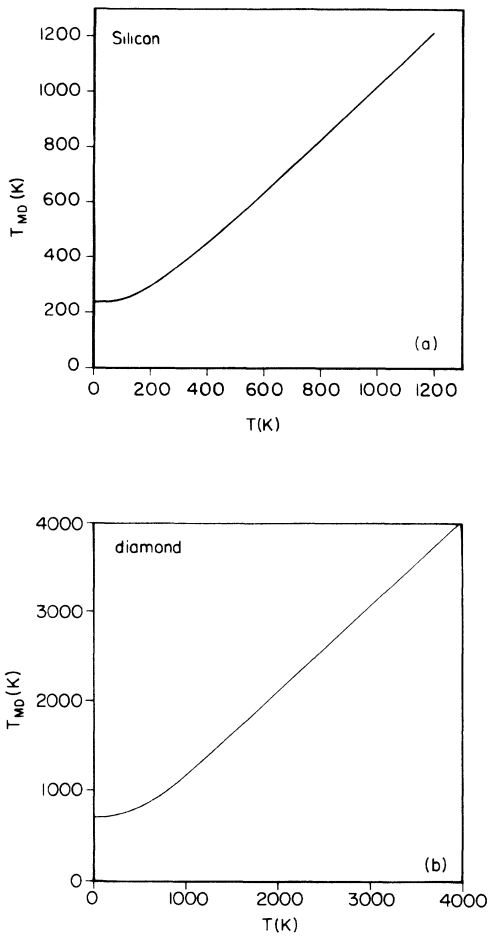

FIG. 2. The scaling relation between the MD averaged temperature T_{MD} and scaled temperature T for (a) silicon and (b) diamond.

of classical statistical mechanics, quantum corrections for the MD results are necessary, particularly at low-temperature regimes if we want to make quantitative comparison with experimental results. While the exact calculation of quantum correction to the MD results is too complicated for our present calculations, we have adopted a simple way of performing the quantum correction by rescaling the MD averaged temperature T_{MD} to a scaled temperature T determined by requiring the mean kinetic energy of our system to be the same as that of the corresponding quantum system at temperature T (including zero-point motion). This leads to the following scaling relation:

$$T_{\mathrm{MD}}=\frac{1}{k_B}\int h\nu D(\nu)\left[\frac{1}{2}+\frac{1}{(e^{h\nu/k_BT}-1)}\right]d\nu\ , \quad (4)$$

where $D(\nu)$ is the phonon density of states of Si or diamond crystal. The scaling relation between T_{MD} and T for Si and diamond are shown in Fig. 2. The MD temperature T_{MD} and the scaled temperature T approach each other at high temperatures, while at $T=0$, k_BT_{MD} corresponds to the zero-point energy of the system. In what follows, the MD simulation results will be presented with the scaled temperature T unless otherwise specified. We note that our previously published results[7,8] have been presented with T_{MD} as the temperature scale.

IV. RESULTS

A. Phonon frequency shifts and linewidths in Si

Phonon frequency shifts and linewidths in Si have been subjected to extensive experimental and theoretical studies.[1-3,20-22] It therefore serves as the primary example for comparing our theory with experiments and other existing theories.

We present in Fig. 3 our results on the temperature-dependent spectral intensities of the LTO(Γ), TO(X), LOA(X), and TA(X) modes of Si. The shifts in frequencies and the increase in linewidths as the temperature increases are clearly evident in the figure. The shift and the broadening of the transverse acoustic mode are found to be much smaller than those of the optic modes.

In order to compare our molecular-dynamics results with available experimental results, we have estimated the temperature-dependent frequency shifts and linewidths from the phonon spectral intensities (Fig. 3). The frequency shifts have been measured with respect to the corresponding mode frequencies at $T=0$ K (or $T_{\mathrm{MD}}=235$ K). The linewidths have been corrected by subtracting out the additional broadening due to the finite simulation time and smoothing procedure. The resulting frequency shifts and linewidths are plotted in Figs. 4 and 5, respectively, in comparison with the available experimental data for the optic mode at Γ and the

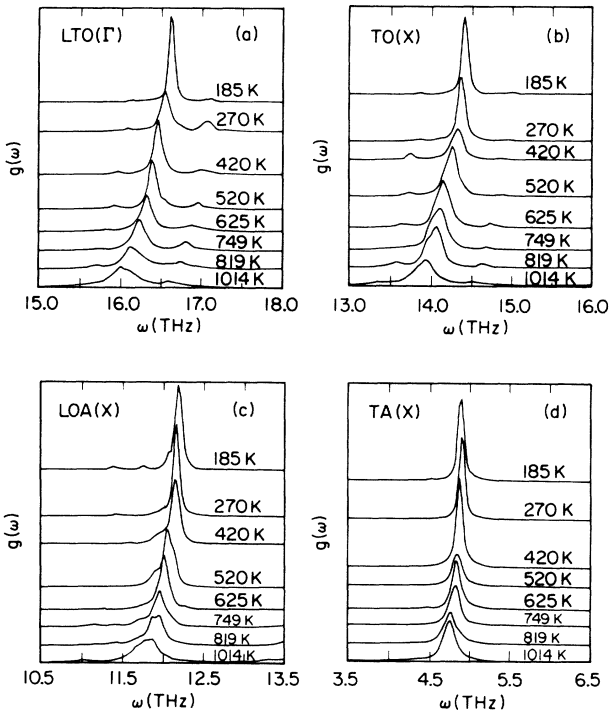

FIG. 3. The temperature-dependent phonon spectral intensities of the LTO(Γ), TO(X), LOA(X), and TA(X) modes of silicon.

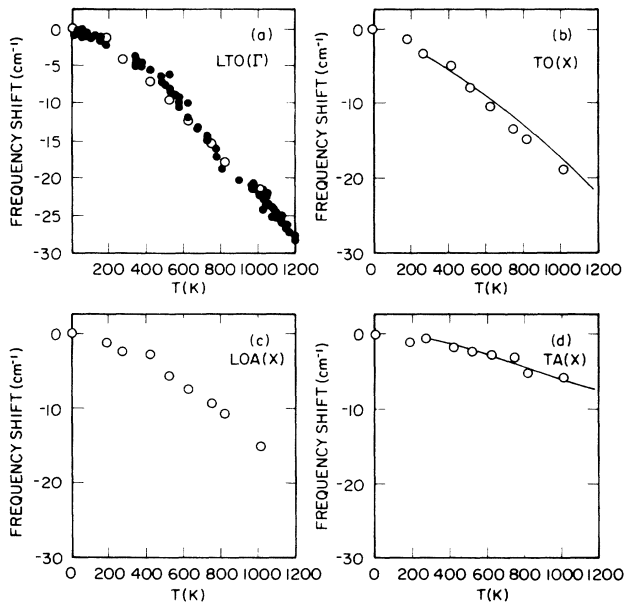

FIG. 4. The temperature-dependent phonon frequency shifts of the LTO(Γ), TO(X), LOA(X), and TA(X) modes of silicon. The open circles are the present TBMD results. The solid dots in (a) are Raman scattering data quoted from Ref. 3. The lines in (b) and (d) are experimental data quoted from Ref. 21.

TO and TA modes at point X. We found that the agreement between the present theory and the experimental data is very good. Some of our molecular-dynamics results do not have existing experimental data for comparison, and we will leave them as theoretical predictions. It should be emphasized that in the present calculations, no input from any experimental data has been used.

B. Phonon frequency shifts and linewidths in diamond

The TBMD results on the phonon spectral intensities of the LTO(Γ), TO(X), LOA(X), and TA(X) modes of

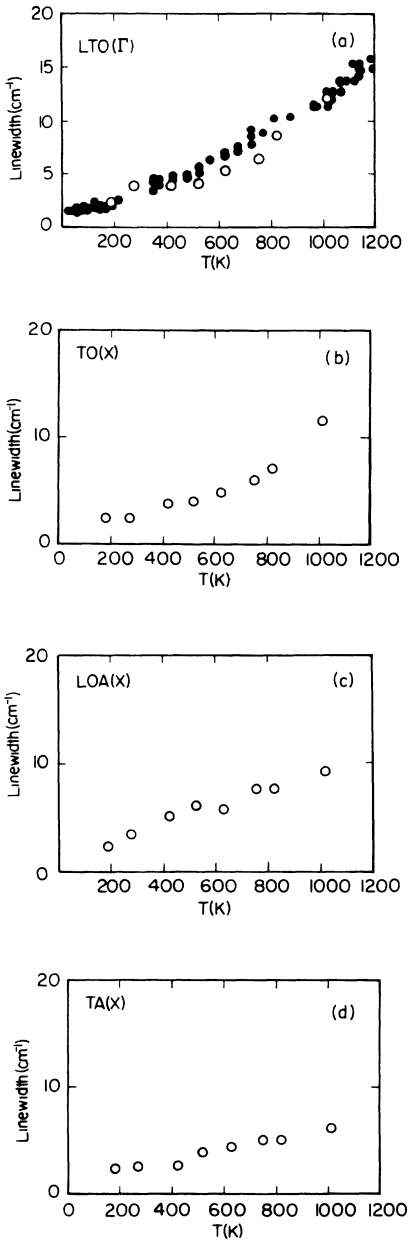

FIG. 5. The temperature-dependent phonon linewidths of the LTO(Γ), TO(X), LOA(X), and TA(X) modes of silicon. The open circles are the present TBMD results. The solid dots in (a) are Raman scattering data quoted from Ref. 3.

diamond are presented in Fig. 6. The phonon frequency shifts and phonon linewidths as a function of temperature are plotted in Figs. 7 and 8, respectively. The general features of the results for diamond are very similar to that of Si. We are not aware of any available experimental data for comparison.

V. DISCUSSIONS

In this section, we wish to discuss further the advantages of the TBMD scheme in comparison with other existing techniques on the subject. In particular, we will compare the molecular-dynamics scheme with the quasiharmonic approximation and the perturbation approach for calculating phonon anharmonic effects and compare the tight-binding force model with empirical classical potential models for molecular-dynamics simulations.

In the quasiharmonic approximation, the temperature dependence of phonon frequency is attributed entirely to the change of force constants due to thermal expansion. The absence of explicit phonon interactions in this approximation generally leads to an underestimate of phonon frequency shift and does not predict phonon lifetimes. In Fig. 9, we compare our molecular-dynamics results with the frequency shifts under quasiharmonic approximation for some zone center and zone boundary modes of Si. The latter have been calculated by frozen phonon calculations with the volume chosen exactly equal to that used in the molecular-dynamics calculation at the corresponding temperature (i.e., thermal expansion included). We found that the quasiharmonic approximation substantially underestimates the frequency shifts. It is interesting to note that the quasiharmonic contribution yields opposite shifts for the TA(X) mode due to the negative Grüneisen constant of this mode.

Perturbative calculation of phonon anharmonic effects in Si have been carried out by Cowley,[2] who determined the harmonic force constants by fitting to the experimen-

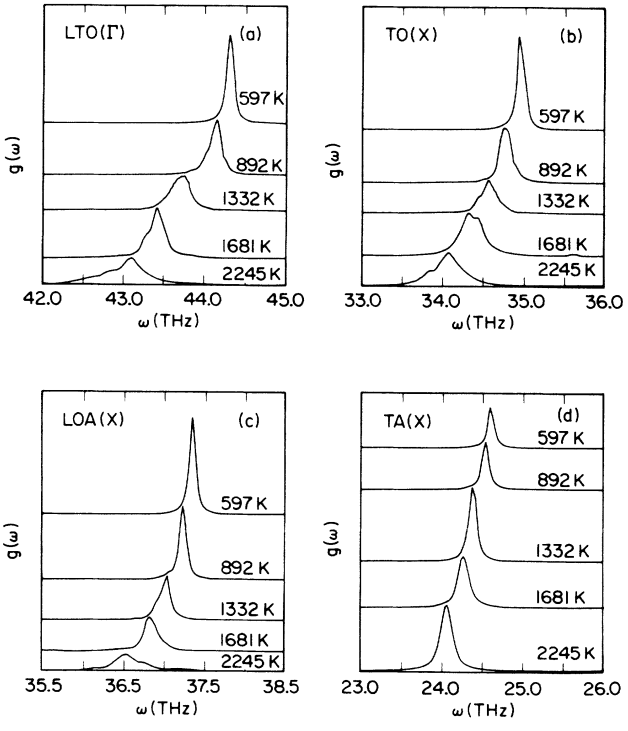

FIG. 6. The temperature-dependent phonon spectral intensities of the LTO(Γ), TO(X), LOA(X), and TA(X) modes of diamond.

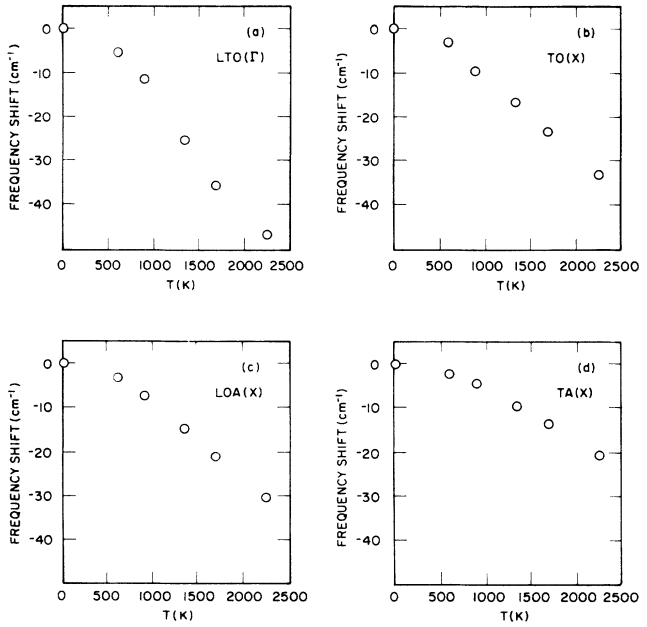

FIG. 7. The temperature-dependent phonon frequency shifts of the LTO(Γ), TO(X), LOA(X), and TA(X) modes of diamond.

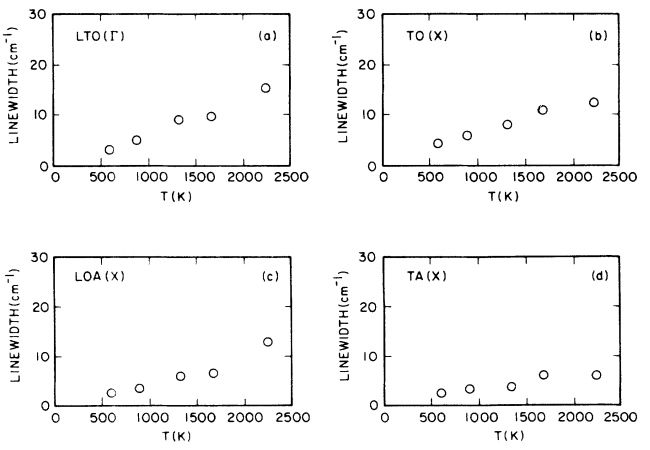

FIG. 8. The temperature-dependent phonon linewidths of the LTO(Γ), TO(X), LOA(X), and TA(X) modes of diamond.

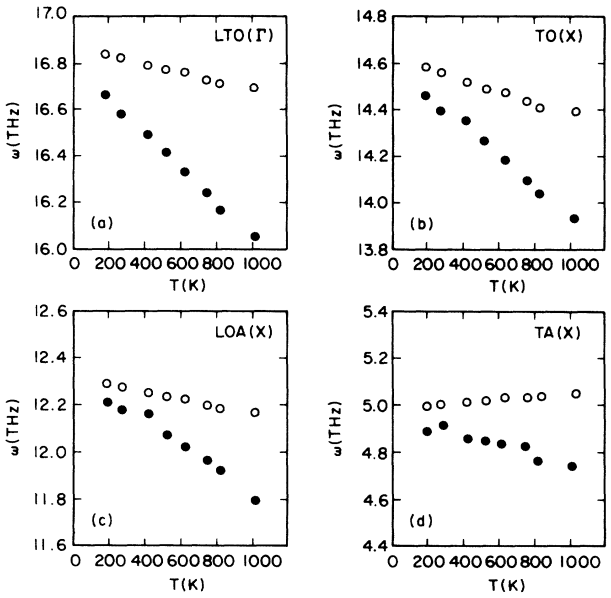

FIG. 9. Phonon frequency shifts in silicon by the quasiharmonic approximation approach (open circles) and by the molecular-dynamics approach (solid circles). The same tight-binding Hamiltonian has been used in both approaches.

tal phonon dispersion and the third-order anharmonic force constants by fitting to the experimental lattice thermal expansion data. Although his results on frequency shifts of the LTO(Γ) mode up to 500 K agree with experiment, no data on higher temperature have been reported. Moreover, the linewidths turned out to be much smaller than Raman scattering data already at $T=500$ K (Ref. 20) indicating that it is necessary to take higher-order anharmonic effects into account for the high-temperature regime. Higher-order perturbations are not only cumbersome in form, but the large number of coupling constants that need to be determined also makes the calculation difficult to perform, while in the molecular-dynamics approach, higher-order anharmonic effects automatically enter through the time correlation functions. Of course one must be able to run the simulation for a reasonably large system for a long enough time. Also the necessity of quantum correction at low temperatures makes molecular-dynamics results less quantitative at low temperatures. However, the approximate scheme of renormalizing the temperature as described in Sec. III seems to do a satisfactory job in extending the molecular-dynamics results from high temperatures to low temperatures in our present calculations.

Recently, there has been a lot of interest in modeling

TABLE V. The Grüneisen parameters of some selected modes of Si obtained by using the present tight-binding model and by using the Stillinger-Weber potential. The corresponding experimental value is also included for comparison.

	Tight-binding	SW Potential	Experiment
$\gamma_{\mathrm{LTO}(\Gamma)}$	0.98	0.80	0.98
$\gamma_{\mathrm{TA}(X)}$	−1.12	−0.04	−1.40
$\gamma_{\mathrm{TO}(X)}$	1.37	0.89	1.50
$\gamma_{\mathrm{LOA}(X)}$	1.02	0.83	0.90

the interatomic interactions in Si by including three-body interactions in classical force models. Among the proposed classical potentials[23–27] for Si the Stillinger-Weber potential[23] seems to be more widely adopted and it has also been reported[28] that it yields the best harmonic properties of Si among its counterparts. However, there have been no reports on the anharmonic properties of Si using the Stillinger-Weber potential or other classical potentials. For the purpose of comparison, we have calculated the mode Grüneisen parameters for the LTO(Γ), TA(X), TO(X), and LOA(X) modes of Si using the Stillinger-Weber potential. The results are listed in Table V in comparison with our tight-binding results and with experimental values. We see that the Stillinger-Weber potential gives fairly poor descriptions for the anharmonic behavior of Si. In particular, the strong negative Grüneisen parameter for the TA(X) mode is well reproduced by the tight-binding model, while the Stillinger-Weber potential gives an almost zero Grüneisen parameter for this mode. We believe that the tight-binding force model provides a much more accurate description of the interatomic interactions in crystalline Si than the Stillinger-Weber potential.

In conclusion, we have shown that the tight-binding molecular-dynamics scheme provides an efficient approach for studying the temperature-dependent anharmonic effects in crystalline tetrahedral semiconductors. We are now testing the applicability of this approach to transition-metal systems, where the d bonding is described by a tight-binding Hamiltonian.

ACKNOWLEDGMENTS

This work is supported by the U.S. Air Force Office of Scientific Research and by the Director of Energy Research, Office of Basic Energy Sciences including a grant of computer time on the Cray computers at the Lawrence Livermore Laboratory. Ames Laboratory is operated for the U.S. Department of Energy by Iowa State University under Contract No. W-7405-ENG-82.

[1]See, for example, *Semiconductors: Physics of Group IV Elements and III-V Compounds,* Landolt-Börnstein New Series III/17a, edited by O. Madelung, M. Schultz, and H. Weiss (Springer-Verlag, Berlin, 1982); *Semiconductors: Intrinsic Properties of Group IV Elements and III-V, II-VI and I-VII Compounds,* Landolt-Börnstein New Series III/22a, edited by O. Madelung, and M. Schultz (Springer-Verlag, Berlin, 1987), and references therein.

[2]R. A. Cowley, J. Phys. (Paris) **26**, 659 (1965).
[3]M. Balkanski, R. F. Wallis, and E. Haro, Phys. Rev. B **28**, 1928 (1983).
[4]See, for example, D. Vanderbilt, S. G. Louie, and M. L. Cohen, Phys. Rev. Lett. **53**, 1477 (1984).
[5]H. R. Glyde, J. P. Hansen, and M. L. Klein, Phys. Rev. B **16**, 3476 (1977).
[6]J. P. Hansen and M. L. Klein, Phys. Rev. B **13**, 878 (1976).
[7]C. Z. Wang, C. T. Chan, and K. M. Ho, Phys. Rev. B **39**, 8592 (1989).
[8]C. Z. Wang, C. T. Chan, and K. M. Ho, Phys. Rev. B **40**, 3390 (1989).
[9]F. S. Khan and J. Q. Broughton, Phys. Rev. B **39**, 3688 (1989).
[10]D. J. Chadi, Phys. Rev. B **29**, 785 (1984).
[11]D. J. Chadi and R. M. Martin, Solid State Commun. **19**, 643 (1976).
[12]W. A. Harrison, *Electronic Structure and the Properties of Solids* (Freeman, San Francisco, 1980).
[13]M. T. Yin and M. L. Cohen, Phys. Rev. B **26**, 3259 (1982); K. J. Chang and M. L. Cohen, *ibid.* **31**, 7819 (1985).
[14]J. R. Chelikowsky and S. G. Louie, Phys. Rev. B **29**, 3470 (1984).
[15]J. H. Rose, J. Ferrante, and J. R. Smith, Phys. Rev. Lett. **47**, 675 (1981).
[16]O. H. Nielsen and R. M. Martin, Phys. Rev. B **32**, 3798 (1985).
[17]In molecular-dynamics simulations, the velocity-velocity correlation function acts as a probe for the phonon excitations of the system even when the dynamics of the system are determined by interatomic potentials, which are not necessarily harmonic [see, for example, R. Car and M. Parrinello, Phys. Rev. Lett. **60**, 205 (1988), in which the velocity-velocity correlation function has been used to calculate the phonon density of states of amorphous silicon]. The spectral distribution of the one-phonon contribution in both Raman scattering (see Ref. 18) and neutron scattering (see Ref. 19) can be related to the Fourier transform of the displacement-displacement correlation function $\langle \mathbf{u}_n(t)\cdot\mathbf{u}_0(0)\rangle$. Essentially the argument is as follows: the experimental response is related to time correlation functions of physical variables (e.g., polarization, density) which can be separated formally (by definition) into one-phonon, two-phonon, etc., contributions by expanding the physical variable in a power series of the displacements. Such a separation is meaningful as long as phonons are still resonably well-defined excitations of the system, i.e., when the spectral density gives a well-defined peak. The Fourier transform of the velocity-velocity correlation function as defined in Eqs. (3) is related to the Fourier transform of the displacement-displacement correlation function by a factor of ω^2. As long as one-phonon processes give a well-defined peak in the spectral density, the peak position and linewidth obtained from the velocity-velocity correlation function can be compared with the one-phonon peak position and linewidth measured in experiment.
[18]R. A. Cowley, in *The Raman Effect,* edited by A. Anderson (Dekker, New York, 1971), p. 176.
[19]S. Doniach and E. H. Sondheimer, *Green's Functions for Solid State Physicists* (Benjamin, Reading, MA, 1974), p. 10.
[20]T. R. Hart, R. L. Aggarwal, and B. Lax, Phys. Rev. B **1**, 638 (1970).
[21]R. Tsu and G. Hernandez, Appl. Phys. Lett. **41**, 1016 (1982).
[22]J. Menendez and M. Cardona, Phys. Rev. B **29**, 2051 (1984).
[23]F. H. Stillinger and T. A. Weber, Phys. Rev. B **31**, 5262 (1985).
[24]J. Tersoff, Phys. Rev. Lett. **56**, 632 (1986); Phys. Rev. B **37**, 6991 (1988).
[25]R. Biswas and D. R. Hamann, Phys. Rev. Lett. **55**, 2001 (1985).
[26]B. W. Dodson, Phys. Rev. B **35**, 2795 (1987).
[27]J. R. Chelikowsky, J. C. Philips, M. Kamal, and M. Strauss, Phys. Rev. Lett. **62**, 292 (1989).
[28]E. R. Cowley, Phys. Rev. Lett. **60**, 2379 (1988).